Low-Temperature Phase Transitions in a Biphenyl−Fullerene Single Crystal: A Raman Study

Dimitrios Palles,*,† Alessandra Marucci,‡ Alain Pénicaud,§ and Giampiero Ruani*,†

I.S.M.N. - C.N.R., Bologna Division, via Gobetti 101, 40129 Bologna, Italy, Laboratoire de Physique des Solides, Université Paris-Sud, 91405 Orsay, France, Centre de Recherche Paul Pascal - CNRS, Université de Bordeaux-I, Av. Schweitzer, 33600 Pessac, France

Received: October 31, 2002; In Final Form: March 17, 2003

We have investigated, by means of temperature-dependent vibrational spectroscopy, the properties of neutral single crystals of C_{60} intercalated with biphenyl. Raman scattering results from a biphenyl−C_{60} single crystal in the temperature range 75−300 K are in support of the two reported phase transitions in the material, as determined by X-ray diffraction (at 147 and 212 K). Following the variations of the Raman features of the single components, biphenyl and C_{60}, it is possible to infer the behavior of the two molecules at such temperatures. In particular, at least three of the main biphenyl mode energies and/or intensities plus the C−H Raman band show modifications correlating with the reported phase transition temperatures. From the variation of the relative intensity of two of the modes, a partial tentative qualitative picture of the biphenyl planarity as a function of temperature can be drawn. The behavior of most of the C_{60} mode energies, widths, and intensities correlate with either of the transitions, but not necessarily both. Especially abrupt H_g mode intensity modifications at ∼147 K seem to result from the influence of the corresponding phase transformation on C_{60} electronic transitions, by changing the C_{60} site symmetry.

Introduction

A large number of experimental and theoretical papers on fullerenes have been focused on the dynamical properties of C_{60}, aiming to investigate the intrinsic properties of the molecule, obtain relevant information on the molecule−molecule interaction in the solid state, as well as contribute to an indepth understanding of the superconducting mechanisms in this system (see refs 1 and 2 and references therein). The possibility of tuning the C_{60}−C_{60} distance, as well as the C_{60} local environment, within a crystal has been shown to be fundamental in exploring the physical properties of this very peculiar molecule. Earlier studies of alkali-doped C_{60} reporting the critical superconducting temperature, T_c, to scale with the C_{60}−C_{60} distance, as well as other experimental evidence, suggested an s-wave BCS-like mechanism for superconductivity where T_c increases with the increase of the density of states at the Fermi energy.[1] Intercalating ammonia in C_{60}^{3-} compounds revealed anomalous properties of this material with respect to a BCS-like model. For example,[3] $(NH_3)K_3C_{60}$ is an S = 1/2 localized spin system suggesting that the C_{60}^{3-} compounds are close to a Mott−Hubbard (M-H) insulator and that the insulating−superconducting transition can be driven by local symmetry. In the same way, in $(NH_3)_xNaA_2C_{60}$ (A = K and Rb), T_c decreases with increasing lattice parameter,[4] in contrast to the BCS-like behavior of non ammoniated compounds. As suggested by Capone et al.,[5] strong correlation in doped C_{60} can induce a significant increase of T_c in the proximity of a Mott transition.

In this framework, the possibility of tuning the C_{60}−C_{60} distance as well as the C_{60} cage relative orientation in the solid state, by synthesizing neutral fulleride structures with additional available sites for doping, constitutes a promising tool to investigate and generate materials with appealing electronic properties. A significant number of neutral mixed C_{60} compounds have been reported (for a nonexhaustive list, see, e.g., refs 6 and 7), although little is known about their disorder. The analysis of the disorder in the present biphenyl−fullerene compound $[(C_6H_5)_2]C_{60}$ (abbreviated as 2P−C_{60}, P ≡ phenyl) will allow an evaluation of the influence that the introduction of an organic molecule has on the interactions and orientations of the C_{60} molecules in the solid and will establish the basis for further doping with alkali metals.[8] A great deal of activity is also devoted to crystal engineering via supramolecular preorganization, as, for example, in the case of the preparation of a linear [2 + 2] addition $(C_{60})_n$ polymer without cross-linking from a cocrystallate of C_{60} and a calixarene (self-assembled in strictly linear separated C_{60} columns with no bonding between any of the C_{60} molecules) after some heat and pressure treatment (see ref 9 and references therein).

Both components of the crystal are neutral in the undoped 2P−C_{60}; the absence of a charge transfer is confirmed by ESR measurements.[8] Four different X-ray diffraction methods have been used so far for the single-crystal characterization,[8,10,11] and they have established the existence of two phase transitions in 2P−C_{60} in the 30−300 K temperature range:

(a) Phase I: at temperatures >212 K, the crystal structure is monoclinic *C*2/*m* (with parameters a = 10.424 Å, b = 16.932 Å, c = 10.320 Å, and β = 100.8° as determined at RT). The fullerene molecules exhibit a strong orientational disorder with nearly all possible orientations at room temperature, including orientational correlations between C_{60} cages.[10] The biphenyl molecules appear, on average, flat. The different diffuse

* Corresponding authors. E-mail: dpalles@ism.bo.cnr.it. E-mail: g.ruani@ism.bo.cnr.it.
† I.S.M.N. - C.N.R., Bologna Division.
‡ Université Paris-Sud.
§ Centre de Recherche Paul Pascal - CNRS, Université de Bordeaux-I.

10.1021/jp027359p CCC: $25.00
Published on Web 05/03/2003

TABLE 1: RT Phonon Energies for the Main C_{60} Intramolecular Modes of Pristine C_{60} and 2P−C_{60} Single Crystals, Obtained with the 1.16 eV Excitation Line

single crystal	$H_g(1)$	$H_g(2)$	$H_g(3)$	$H_g(4)$	$H_g(5)$	$H_g(6)$	$H_g(7)$	$H_g(8)$	$A_g(1)$	$A_g(2)$
C_{60}	266	430	709	772	1100	1240	1406	1574	496	1468
	272	435			1110	1245	1418			
						1250	1424			
2P−C_{60}	265	432	709	757	1100	1240	1407	1574	494	1468
	268			772	1110	1245	1417			
	272			783		1250	1424			

scattering features give evidence of (i) a second-order isotropic transition from phase I toward phase II as the correlation lengths along *a*, *b*, and *c* are of the same order of magnitude and increasing with decreasing temperature, (ii) stacking disorder between (*a*, *c*) planes, which seem to possess more than one type of long-range order, (iii) local ordering along [1,0,±1] directions likely due to interactions between 2P and C_{60} and the possible formation of "chains" with a correlation length of ∼50 Å.

(b) Phase II: a second-order phase transition to another monoclinic *I*2/*a* structure (with parameters *a*, *b*, 2*c*) is observed at $T_{C1} \sim 212$ K. The biphenyl appears twisted by ∼23° and adopts two preferential orientations alternating along the *c*-direction. The fullerene orientational order, compatible with the *I*2/*a* symmetry, starts at $T < 212$ K (below the transition) and gradually increases with decreasing temperature (at 155 K, 65% of the C_{60} molecules are ordered in two preferential orientations alternating along the *c*-direction) apparently driven by the biphenyl ordering.

(c) Phase III: a first-order phase transition (accompanied by hysteresis effects) to a triclinic structure (with parameters $a + b$, $a - b$, c, $\alpha = 90.9°$, $\beta = 100.8°$, $\gamma = 90°$) is observed at $T_{C2} \sim 147$ K. The loss, in phase III, of the phase II doubling of parameter *c*, points to a re-ordering of both biphenyl and ordered C_{60} molecules. Fullerene ordering continues in phase III and is completed at $T \sim 100$ K.

We have studied this system using the sensitivity of Raman spectroscopy to gauge slight modifications of the molecular structure and of the local environment of molecules; this investigation allowed us to independently analyze the effect of phase transformations on the single components of the mixed crystal.

Experimental Section

2P−C_{60} single crystals were prepared by slow cocrystallization of a saturated solution of C_{60} and biphenyl in toluene at room temperature.[8]

A series of confocal micro-Raman spectra were recorded through a Renishaw 1000 system (equipped with a Peltier refrigerator-cooled CCD) using the 514.5 nm (2.41 eV) Ar^+ laser line focused on the sample through a ×50 objective lens of 2 μm resolution and 10.8 mm working distance. By using this lens, the diameter of the laser spot on the sample is ∼2−3 μm. The laser power used was in the range of 10−20 μW (power density range of ∼150−350 W/cm^2). Acquisition times were typically 22.5 min, and the spectra were collected in the unpolarized backscattering geometry. The spectrometer resolution is ∼3.2 cm^{-1} for the laser line used. Low temperatures were achieved by means of an open-cycle liquid-helium-flow modified Oxford Instruments cryostat with a temperature stability <0.5 K, mounted on an *xyz* micro stage.

Subsequently, measurements were repeated in a ∼2.0 cm^{-1} resolution FRA 106 Raman module adapted to a Bruker IFS 88 FT interferometer using the NIR 1064 nm (1.16 eV) excitation line, focused on a spot of about 300 μm diameter at a power density of 15−30 W/cm^2. The same cryostat was employed.

For a low-thermal-conductivity material such as C_{60}, the temperature increase is proportional to the inverse of the thermal conductivity and to an effective power defined as (laser power/spot diameter), but not to the power density (= [laser power/(spot diameter)^2]) (see ref 12 and references therein). With the above values for the spot diameter and laser power, the local temperature increase resulting from the laser-induced heating (ΔT) at RT is estimated to be 2−7 K for the micro-Raman spectra, assuming a 2P−C_{60} absorption coefficient at 2.41 eV excitation similar to the one for pristine C_{60}. At lower temperatures, ΔT is even smaller as a consequence of the inverse proportional dependence of the thermal conductivity on the temperature.[13] For FT-Raman spectra acquired with the 1.16 eV excitation at the usual power, the laser heating is expected to be negligible, since both 2P and C_{60} are transparent in this energy region.

Error bars relative to average energies, line widths, and other parameters in the following results represent the experimental error for a single measurement, unless otherwise stated. In the case of the determination of the phonon energy of a well-resolved peak, resulting from a typical fit procedure, this error is usually <0.5 cm^{-1} (smaller than the spectrometer resolution), while the corresponding line width error is larger and depends substantially on the spectrum quality, ranging from <0.5 for very well resolved peaks such as $A_g(2)$ and up to 1−2 cm^{-1}.

Room-temperature infrared (IR) absorption measurements were performed by using a Bruker IFS 88 FT interferometer equipped with a microscope of a spatial resolution of 30 μm.

Results

Due to the lower crystal lattice monoclinic symmetry in 2P−C_{60} (*C*2/*m* and *I*2/*a*), as compared to both the pristine C_{60} RT fcc phase (*Fm*3*m*) and the low-temperature sc phase (*Pa*3), one would expect a more extensive splitting of the molecular C_{60} $2A_g + 8H_g$ Raman active modes, according to the reduction of symmetry. On the other hand, as in the case of the pure C_{60} crystal, rapid rotations of fullerenes at RT and down to at least ∼212 K would be expected to smear out the effects of the crystal field splitting on vibrational modes.

The superposition of these two competing effects at RT, as evidenced through the Raman spectra obtained by exciting 2P−C_{60} in the NIR at 1.16 eV, shows that the I_h C_{60}-derived $H_g(1)$, $H_g(2)$, $H_g(3)$, and $H_g(4)$ Raman active modes behave differently with respect to pristine C_{60} (see Table 1): (a) the $H_g(1)$ and $H_g(4)$ modes split into three peaks, as opposed to the $H_g(1)$ doublet and the $H_g(4)$ single peak in the C_{60} fullerite, and (b) the $H_g(2)$ and $H_g(3)$ mode line widths are ∼50% narrower than those of their C_{60} counterparts. In the case of the $H_g(1)$ and $H_g(6)$ modes, one of the three peaks is hardly seen at RT and thus the splitting of the two strongest peaks is ∼7 cm^{-1} for

TABLE 2: RT Phonon Energies for the Strongest 2P Modes of Pristine 2P (after ref 25) and 2P−C_{60} (this work) Single Crystals[a]

	$A_g(11)$	$A_g(10)$	$A_g(9)$	$A_g(8)$	$A_g(7)$	$A_g(6)$	$A_g(4)$
2P single crystal	315	742	1003	1030	1190	1285	1612
2P−C_{60} single crystal	324	740	1004	1032	1152	1275	1607

[a] The mode assignment is also reproduced from ref 25.

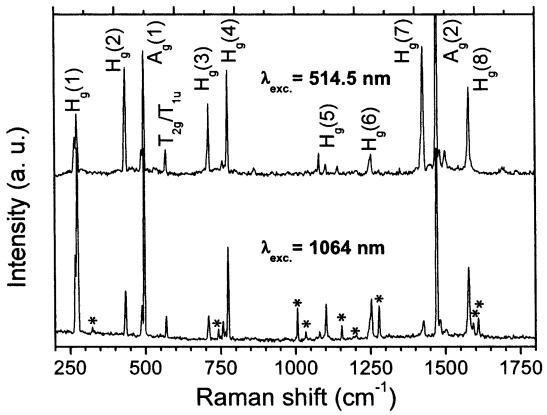

Figure 1. 2P−C_{60} Raman scattering spectra recorded at 125 K exciting at $\lambda_{exc} = 514.5$ nm (2.41 eV) and $\lambda_{exc} = 1064$ nm (1.16 eV). 2P peaks are denoted by stars.

both of these modes, but the existence of the third component is also confirmed by the spectra at lower temperatures (Figure 1). The A_g modes exhibit red- or blue-shifted satellite peaks as in the C_{60} fullerite. However, the strongest peak energies of all modes retain their pristine fcc C_{60} RT values[14] within ± 2 cm^{-1}.

A. Micro-Raman Spectra @2.41 eV. The 2.41 eV excitation falls into an absorption region of C_{60} around the first dipole-allowed transition at 2.4−2.7 eV in C_{60} thin films and single crystals, and thus the fullerene electronic structure is at pre-resonant conditions.[15] This is probably the reason only C_{60} modes can be observed in the spectra (Figure 1): the 2P spectrum is screened by the fullerene (see Discussion section).

In Figure 2, the temperature dependence of the spectral parameters (intensity, mode energy, and line width) of the most pronounced C_{60} Raman modes in the 2P−C_{60} system is reported together with literature data obtained from pristine C_{60}[15] and *n*-pentane clathrate C_{60}.[16] At temperatures $T < T_{C1}$ (~212 K), the Raman spectra are very similar to pristine C_{60} spectra (see, for example, ref 15). As the temperature is lowered below T_{C2} (~147 K), the most notable change is the strong intensity enhancement, mainly of H_g modes. The $H_g(2)$ and $H_g(7)$ are the modes that appear to be influenced most: their relative intensity (with respect to the 75 K values) decreases by at least a factor of 10 between 75 and 200 K. The relative intensity of the $A_g(1)$ mode decreases by a factor of 5 between 75 and 250 K, which is approximately twice as much compared to pristine C_{60}, whereas the $A_g(2)$ mode lies closer to the pristine C_{60} behavior. It is noteworthy that practically all of the mode relative intensities show modifications at the phase transitions around 150 and 200 K as well as at 90 K. The most evident are the cases of $A_g(1)$ and $H_g(7)$ (Figure 2a).

Besides the strong relative intensity variations of C_{60} modes in the range 75−240 K, other mode features show modifications at either or both T_{C1} and T_{C2}. The $A_g(1)$ mode softens by ~1 cm^{-1} at $T \sim T_{C1}$, while the $A_g(2)$ shows a sharp dip at $T \sim T_{C2}$ (error bars for the computed energy are smaller than 1 cm^{-1}) and a slope change at $T \sim T_{C1}$ (Figure 2b). The $H_g(8)$ mode

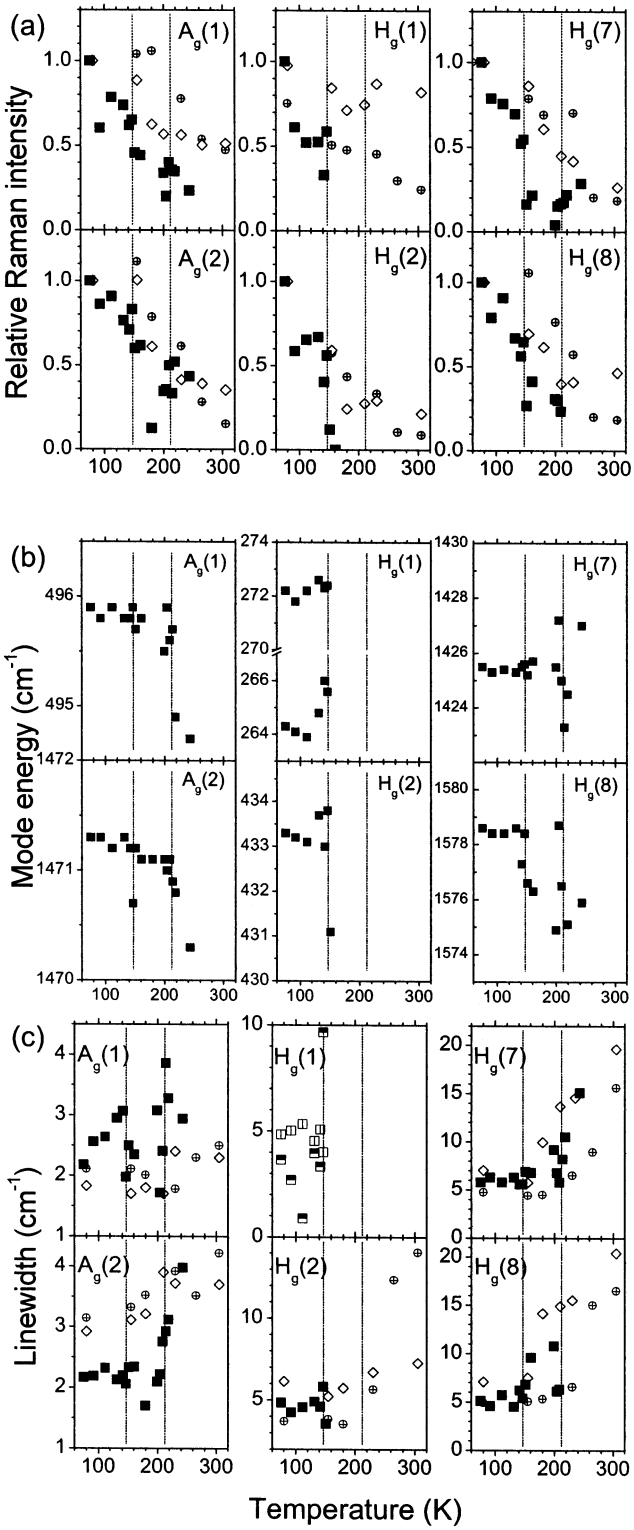

Figure 2. Comparison of the temperature evolution of the characteristic parameters for the 2P−C_{60} (black filled squares) A_g and some of the H_g modes with data taken from literature for pristine C_{60}[15] (open crossed circles) and *n*-pentane clathrate C_{60}[16] (open diamonds): (a) relative peak intensities with respect to the 75 K spectra; (b) mode energies; (c) mode line widths. 2P−C_{60} single-crystal unpolarized Raman spectra were acquired using the 2.41 eV (514.5 nm) Ar^+ line in the backscattering geometry. The typical total time per spectrum was 22.5 min. Vertical lines correspond to 2P−C_{60} transitions.

energy is observed to behave rather discontinuously across both T_{C1} and T_{C2}, whereas $H_g(7)$ is influenced only across T_{C1}. The $H_g(2)$ is characterized by a strong abrupt softening for $T > T_{C2}$.

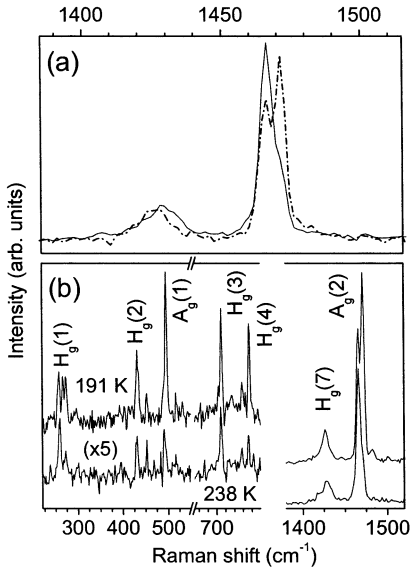

Figure 3. (a) Initiation of phototransformation evidenced from the modification of the $A_g(2)$ mode spectral region of the 2P−C_{60} single crystal for a fast (4.5 min; dot−dash line) and a longer (22.5 min; solid line) unpolarized Raman spectrum at a power density of ∼250 W/cm^2. (b) Partial recovery of the monomer C_{60} phase of the 2P−C_{60} single crystal upon cooling from ∼238 K (lower curve) to ∼191 K (upper curve) as evidenced in 2P−C_{60} single-crystal unpolarized Raman spectra.

The occurrence of two phase transitions is detected by the behavior of mode line widths as well. The changes between one phase and another can be of the order of 100% (Figure 2c). The $A_g(1)$ mode line width is discontinuous across both T_{C1} and T_{C2}, with values exceeding the pristine C_{60} ones, except at the temperatures of the phase transitions. The $A_g(2)$ line width is practically constant for $T < T_{C1}$ with values ∼35% lower than the pristine C_{60} ones, before it starts its steep rise at $T \sim$ 200 K to reach pristine C_{60} values at $T \sim$ 240 K. The $H_g(8)$ line width shows two clear transitions at $T \sim$ 150 K and $T \sim$ 200 K, with phase II values being twice as large with respect to pristine C_{60} (Figure 2c). The $T \sim T_{C2}$ transition is obscured in the $H_g(7)$ line width trend.

Phototransformation of pristine C_{60} at sufficiently high power density (>5 W/cm^2 for 514.5 and 488.0 nm lines[17]) has been extensively studied (for a review, see for example, ref 18). The phototransformation of 2P−C_{60} is observable above 212 K (see also the Discussion section), accompanied by the development of cracks on the single-crystal surface around the region of the laser illumination. Because of the low scattering signal from the sample inside the cryostat, it was not possible to further lower the laser intensity, so as to avoid photoinduced effects for $T >$ 212 K. The spectrum of the phototransformed crystal is very similar to the one of the dimer phase $(C_{60})_2 \equiv C_{120}$,[19] apart from a shift of 3−4 cm^{-1} for most modes. Figure 3a shows that a longer accumulation time at ∼221 K allows the photoinduced $A_g(2)$ dimer band to develop up to the almost complete disappearance of the monomer structure.

A different aspect of the process is shown in Figure 3b: starting from the photodimer at ∼238 K, the C_{60} monomer band develops a very strong component upon cooling to ∼191 K (after letting the system stabilize for 3 h), while the photodimer scattering intensity slightly decreases.

B. FT-Raman Spectra @ 1.16 eV. In the case of the 1.16 eV excitation, nonresonant conditions for both C_{60} and 2P are guaranteed (for 2P thin films the absorption edge is close to 4.1 eV[20]); thus, the advantage over the 2.41 eV excitation lies in the observation of the modes of both types of molecules in the spectra (Figure 1). Changes are observed at crossing both transition temperatures.

Raman spectra of oligophenyls have been described by several authors (see, for example, ref 21 and references therein) and are dominated by four groups of totally symmetric (A_g, A_1, or A, depending on the molecular conformation) modes. One doublet, ν_2, in the 1200−1300 cm^{-1} range (1220 and 1280 cm^{-1} peaks) that was assigned to a combination of strong C−H in-plane bending plus C−C inter-ring stretching vibrations[22] has drawn particular interest. The Raman intensity ratio (I_{1280}/I_{1220}) of these peaks has been observed to be inversely proportional to the number of phenyl rings in the chain, but at the same time is also an indicator of planarity, since simulations show that a higher number of conjugated phenyl rings results in a lower torsional angle, τ, between them.

For 2P, (I_{1280}/I_{1220}) ≈ 25, while for oligo-*p*-phenylenes beyond 6P, (I_{1280}/I_{1220}) ≈ 1. The behavior of this mode intensity ratio as a function of temperature or hydrostatic pressure, for oligo-*p*-phenylenes, has been directly correlated to the variation of the inter-ring tilt angle as a function of the same external parameters: indeed, a reduction of the average inter-ring tilt angle with increasing temperature and even planarisation upon application of pressure was observed.[23] In a similar fashion, the Raman intensity ratio between the components of another doublet, at 1595 and 1610 cm^{-1}, was experimentally observed to correlate with the reported phase transition in pristine 2P at $T \sim$ 40 K, in which the torsional angle between the two phenyl rings is decreasing for $T >$ 40 K.[24] This doublet, ν_1, was assigned to a combination of C−C double-bond stretching, single-bond shortening (including the inter-ring bond) plus C−H in-plane bending vibrations[22]—but contrary to the case of terphenyl, in 2P the splitting can be assigned to a Fermi resonance of ν_1 with some overtone or combination and not to a fundamental frequency (see ref 22 and related references therein).

The 2P Raman spectrum of 2P−C_{60} exhibits four strong A_g modes at 1004, 1152, 1275, and 1607 cm^{-1}, weak modes at 324, 740, 1032, and 1590 cm^{-1}, and even weaker ones at 163, 545, 611, and 1201 cm^{-1} (see Figure 1 for a 125 K spectrum), plus C−H stretching modes in the region 2950−3150 cm^{-1} (Figure 4). We identify the ∼1275 and ∼1200 cm^{-1} peaks as the ν_2, and the ∼1590 and ∼1610 cm^{-1} peaks as the ν_1 doublet, respectively.

The energies of the two strong components of the ν_2 and ν_1 modes, respectively, at ∼1275 and ∼1610 cm^{-1}, clearly show modifications at both T_{C1} and T_{C2} (Figure 5). The ∼1275 cm^{-1} mode upshifts rather discontinuously in phase II, while the few data points for the weak ∼1200 cm^{-1} mode show that it behaves in the opposite way. The ∼1610 cm^{-1} mode upshifts rather discontinuously only for $T \sim$ 147 K, while the weak ∼1590 cm^{-1} mode changes are not correlated with only T_{C2} or T_{C1}. Contrary to the ab initio calculations of ref 22, the ∼1275 cm^{-1} mode is stronger than the ∼1610 cm^{-1} one, and additionally its peak happens not to overlap with C_{60} modes, unlike the ν_1 doublet. Thus, it is better resolved in the spectra and its line width variation, as a function of temperature, shows a discontinuous change at $T \sim$ 210 K diminishing from 6 to about 4 cm^{-1}.

The relative intensity ratios (I_{1275}/I_{1200}) and (I_{1590}/I_{1610}) have nonnegligible error bars that are partly due to low statistics (especially for the 1200 cm^{-1} peak) and partly to the possible superposition of low-intensity C_{60} $H_g(8)$ split bands overlapping with the ν_1 doublet. We therefore chose to use the integrated

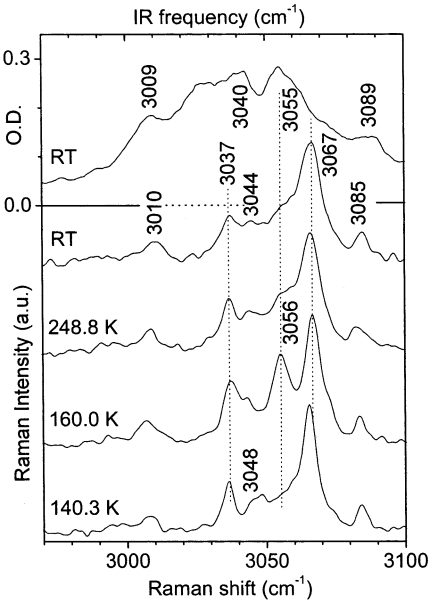

Figure 4. Temperature evolution of unpolarized Raman spectra acquired in backscattering geometry using the 1.16 eV excitation line, plus room-temperature IR absorption spectrum of the C−H stretching vibrations spectral region.

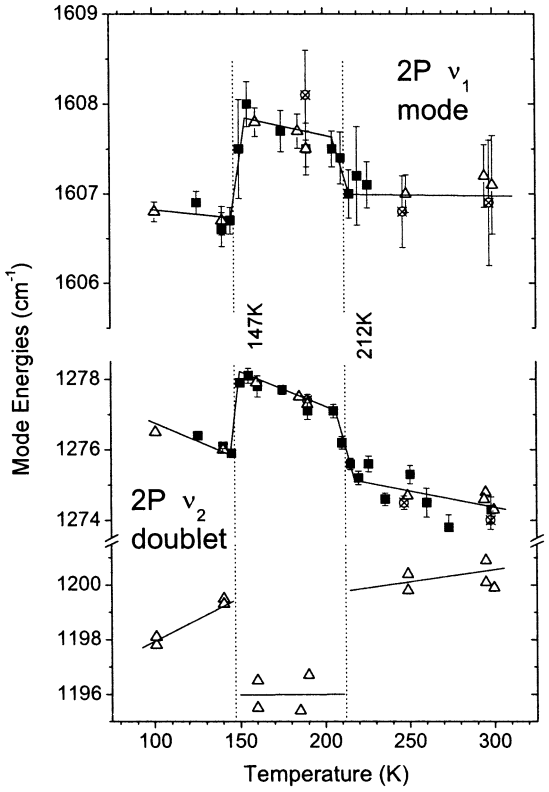

Figure 5. Temperature dependence of three 2P mode energies. Phase transition temperatures are indicated by vertical dotted lines. Different symbols correspond to different sets of measurements. The lines are guides to the eye.

intensity ratio of the ν_1 or ν_2 doublet with respect to the total C−H 2930−3200 cm^{-1} stretching band. This band was suggested as an internal standard for calibration of experimental Raman intensities of *p*-phenylene oligomers, useful for structural studies, because its intensity does not substantially change with τ; ab initio calculations show that the band intensity increases only slightly when the 2P molecule passes from the planar ($\tau = 0°$) to the $\tau = 90°$ twist conformation.[22] The above-mentioned

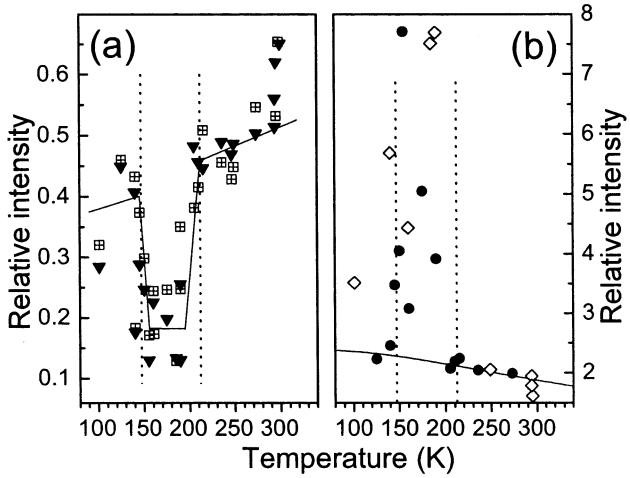

Figure 6. (a) Temperature dependence of the relative intensities ($I_{\nu 2}/I_{C-H}$) (crossed squares) and ($I_{\nu 1}/I_{C-H}$) (filled black down triangles); the lines are guides to the eye; phase transition temperatures are indicated by vertical dotted lines. (b) Temperature dependence of the intensity ratio ($I_{C-H}/I_{\nu 1}$). The solid line is a fit to the data of phases I and III using eq 1, where the activation energy is kept fixed at 0.04 eV.[21] Different symbols correspond to different sets of measurements. Phase transition temperatures are indicated by vertical dotted lines.

intensity ratios, $I_{\nu 1}/I_{C-H}$ and $I_{\nu 2}/I_{C-H}$, in these calculations are seen to diminish when the torsion angle increases. This is exactly what is observed in Figure 5, where a clear lowering of the values corresponds to phase II. Assuming that the inverse ratio, $I_{C-H}/I_{\nu 1}$, is proportional to the probability for the system to be in a nonplanar configuration, that the potential energy of the two 2P rings is a "W"-shaped function of the torsion angle, and that the planar/nonplanar conformational change is thermally activated,[21] we performed a fit to the data of phases I and III using

$$I_{C-H}/I_{\nu 1} = A[1 - \exp(-\Delta E_{np \rightarrow p}/k_B T)] \qquad (1)$$

but fixing $\Delta E_{np \rightarrow p} = 0.04$ eV as derived in ref 21 for the ratio of the two components of the ν_2 doublet. The fit in Figure 6b satisfactorily describes the data of phases I and III, but not those of phase II.

The reduction of symmetry related to the distorted structure of the 2P, and consequently the modification of Raman features, is perhaps most impressive in the C−H stretching bands in the 3040−3080 cm^{-1} region. In Figure 4, the Raman spectra of this region recorded in the temperature domains of the three phases are compared with the room-temperature IR absorption spectrum. The reduction of symmetry in phase II, is evidenced by the observation of a clear additional component at ∼3055 cm^{-1}, which is absent in both phases I and III (Figure 6) and corresponds to a Raman forbidden IR active mode.

Discussion

A. Behavior of C_{60} in the Mixed Crystal. The 2.41 eV laser excitation line lies in the pre-resonant region of the optically forbidden h_u-t_{1u} (free C_{60} level labeling) electronic transition. This may have a nonnegligible effect on nontotal symmetric modes, such as the H_g ones, which are sensitive to the Herzberg−Teller resonant Raman enhancement and may gain scattering cross section even from forbidden transitions. This effect has already been observed in pristine C_{60} as well as in other charge transfer (e.g., A_xC_{60}[14]) or noncharge-transfer compounds (e.g., *n*-pentane C_{60} clathrate[16]).

The intensity enhancement of C_{60} Raman modes with decreasing temperature was correlated with the orientational ordering of C_{60} in solids.[15] Especially the Raman intensity of the H_g modes appears very sensitive to subtle changes of the band structure as a result of the specific vibrational mixing of electronic states (bands in the case of solid C_{60}).

The C_{60} H_g modes scattering intensity enhancement in 2P−C_{60} for $T < 147$ is reminiscent of the C_{60} or clathrate−C_{60} behavior across the corresponding C_{60} orientational phase transition. We are thus led to conclude that the observed phase transitions in 2P−C_{60} must also be related to the C_{60} orientational ordering. The deviations of the results of 2P−C_{60} with respect to the pristine C_{60} results constitute evidence of the influence of 2P on the electronic band structure of C_{60} in 2P−C_{60}. The line width temperature dependence of most of the C_{60} Raman active modes shows a discontinuity at T_{C1}, as observed in the pristine C_{60} in coincidence with the transition from the face-centered to the simple cubic crystal structure.[26] This confirms the strong reduction of C_{60} free rotation also in 2P−C_{60}.[10]

The C_{60} photodimerization under excessive laser illumination is understood to be occurring in the (*a*, *b*) plane along the shortest center-to-center distance (9.94 Å), which is approximately 1% smaller than the fcc C_{60} one (10.02 Å). In close analogy, the heat- and pressure-treatment-induced linear [2 + 2] addition $(C_{60})_n$ polymerization in a cocrystallate of C_{60} and a calixarene is understood to be occurring along the 9.92 Å center-to-center distance within each calixarene columnar stack-separated fullerene column.[9]

Despite the shorter nearest-neighbor C_{60} molecule distance, no polymerization occurs below 212 K. This is probably a result of the freezing of the rotational degrees of freedom in a way similar to that of pristine C_{60} where the double bonds in one cage end up facing pentagon or hexagon centers of the adjacent cage.[18,27] The exclusion of the probability for two adjacent cages C−C double bonds to face each other results in the frustration of light-induced 2 + 2 cycloaddition-type reactions. Moreover, the reemergence of the monomer in the spectrum, by lowering the temperature below T_{C1} and letting the system relax for more than 2 h, is probably a consequence of the high instability of the dimer that is broken apart, even by the small thermal energy corresponding to a temperature of ∼200 K. Above T_{C1}, the photogeneration rate is larger than the thermal dissociation one and 500 s of exposure are enough to completely phototransform the illuminated portion of the sample; below T_{C1}, the phototransformation is inhibited and the system can return over time to the pristine structure.

The case of 2P−C_{60} is a good opportunity to compare the effect of the C_{60} site symmetry lowering (from O_h in RT pristine C_{60} to C_{2h}) and the corresponding crystal field on the C_{60} modes, in the absence of charge transfer. In the case of M_6C_{60} (C_{60} site symmetry T_h), where the charge state of the fullerene is C_{60}^{6-}, at least six K_6C_{60} H_g bands split in E_g + T_g doublets at RT, although the effect is dependent on the excitation energy and is diminished when exciting in the 1.16 eV NIR line.[14] In 1.16 eV-excited 2P−C_{60}, as already mentioned, nearly all H_g bands split in three. The RT $H_g(2)$ does not show splitting, but at lower temperatures and with a laser excitation at 2.41 eV a low-frequency shoulder appears—similarly the RT $H_g(3)$ mode splitting is perceived as a low-frequency asymmetry. In particular, the results on the $H_g(1)$ mode have shown that the splitting of the mode depends on the alkali metal.[14] Although in the case of charge transfer this splitting also depends on the Jahn−Teller effect,[28] the fact that the splitting of the same mode

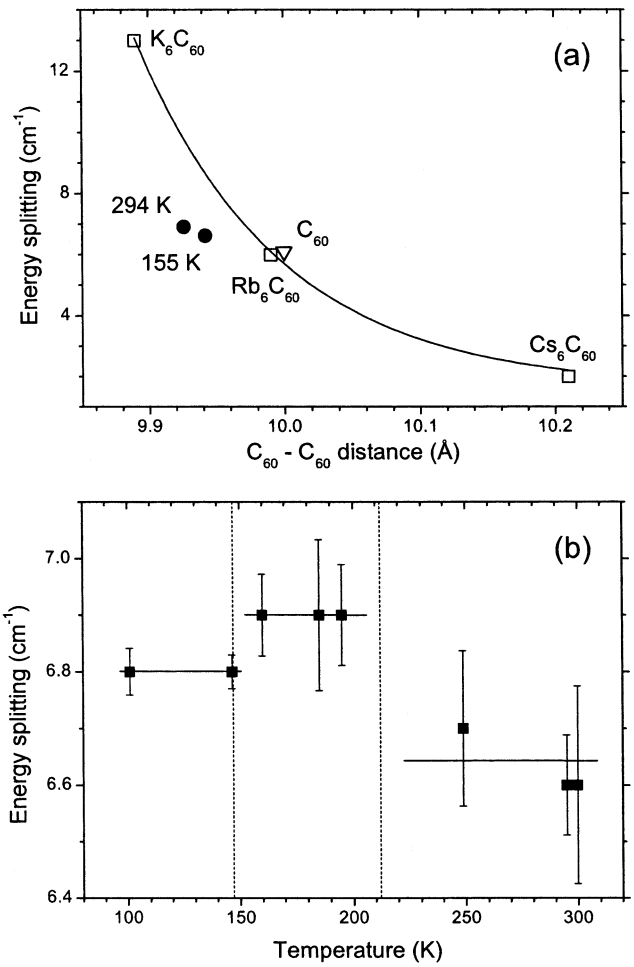

Figure 7. (a) Dependence of the splitting of the $H_g(1)$ mode on the C_{60}−C_{60} inter-cage distance of some fullerides[29−31] (open symbols). In the case of 2P−C_{60}, the shortest C_{60}−C_{60} distances for RT and 155 K are used (black filled circles). (b) Temperature dependence of the splitting of the two strongest $H_g(1)$ modes of C_{60} in 2P−C_{60}. Raman spectra in the backscattering geometry using the 1.16 eV laser excitation. Phase transition temperatures are indicated by vertical dotted lines.

in RT fcc C_{60},[29−31] as well as 2P−C_{60}, scales with the C_{60}−C_{60} distance (Figure 7a) (in the case of 2P−C_{60} the shortest distance is used[8]) indicates that the crystal field strength in 2P−C_{60} is higher than in the pristine fullerite. Along the line of discussion in ref 16, this is confirmed by the stronger enhancement of the H_g mode intensities at lower *T*, or equivalently, by the stronger suppression of the relative intensities of these modes with increasing *T*, with respect to pristine fullerite, as clearly seen in Figure 2a. In the temperature dependence of the $H_g(1)$ splitting shown in Figure 7b, the changes are within the experimental error limits and thus do not allow a definite interpretation, although small shifts at the phase transition temperatures cannot be excluded.

B. Behavior of 2P in the Mixed Crystal. The 1.16 eV excited Raman spectra of 2P−C_{60} single crystal versus temperature give evidence of changes of the torsion angle between the two phenyl rings of the 2P molecule in the different crystallographic phases. In principle, one could estimate values of the torsion angle τ of 2P by comparing the relative changes of the intensity ratio $I_{\nu 1}/I_{C-H}$ experimentally obtained with those obtained by ab initio calculations.[22] The average relative increase of the experimental $I_{\nu 1}/I_{C-H}$ ratio at room temperature ($\tau \sim 0°$) with respect to phase II ($\tau \sim 23°$) is significant (∼100% for 2P in 2P−C_{60}), while the corresponding calculated increase for a

twist from $\tau \sim 23°$ to $\tau \sim 0°$ for a 2P molecular crystal is ~20%. The comparison is obtained by considering, as suggested in ref 22, the integrated intensity in the C−H stretching region as almost constant with respect to τ. In this way, the intensity ratio is probably overestimated. In fact, this does not take into account the temperature dependence of the Raman scattering intensity. Moreover, the strong increase in the Raman spectrum (more than 15% of the total Raman intensity above 3000 cm^{-1}) of one of the IR active components of the C−H stretching in phase II ($\tau \sim 23°$) has not been considered (this would cause a correction toward higher $I_{\nu 1}/I_{C-H}$ values for phase II).

The line width behavior of the stronger ~1275 cm^{-1} mode of the ν_2 doublet may be understood by making the following considerations. Since the time scale in Raman scattering is approximately 8 orders of magnitude smaller than the oscillations of the phenyl rings (5 MHz, see ref 32), Raman spectra are "snapshots" of the oscillating phenyl rings. Above ~190 K, the approximately constant value of the ~1275 cm^{-1} mode line width may be a result of the enhanced thermal motion of the rings that apparently results in a wider distribution of possible τ-values for the phenyl scatterers at any Raman instant. For $T < 190$ K instead, the accessible τ-values may well be more limited as a result of "freezing" effects and consequently the modes substantially influenced by ring torsions would be expected to narrow down in line width with decreasing temperature. The same arguments would then be applicable to the behavior of the ~1610 cm^{-1} mode line width (Figure 5b).

It has been shown that in the low-temperature phase ($T < 40$ K, $\tau \approx 10°$) of the 2P crystal, the intensity ratio between the two ν_1 components (I_{1590}/I_{1610}) is larger than 1 and it decreases to approximately 0.3 at room temperature ($\tau \approx 0°$).[24] Despite the larger torsion angle between the two phenyl rings observed in phase II of the 2P−C_{60} single crystal ($\tau \approx 23°$) with respect to the molecule in the pure 2P crystal at low temperature, the I_{1590}/I_{1610} ratio we have measured for this system at different temperatures is almost constant in all three structural phases (0.34−0.37 phase III, 0.46−48 phase II, 0.37−0.42 phase I) of the 2P−C_{60} compound. This behavior is probably related to the different chemical pressure in the three directions of the 2P molecule in the two crystals (pure 2P in contrast to 2P−C_{60}); in fact, the strong dependence of the I_{1590}/I_{1610} ratio on the inter-ring bond length as well as the strong compressibility of the latter can completely modify the behavior of this observable with respect to only a single parameter such as the torsion angle τ. As a consequence it is not possible to use this intensity ratio to determine the torsion angle.

The unambiguous behavior of the C−H band Raman spectra (Figure 6) that differentiates phase II from the other two phases may very simply be attributed to the symmetry lowering—i.e., strong departure from inversion symmetry and the activation of the IR mode at 3056 cm^{-1}. This scheme would be in accordance with a strong out-of-plane distortion of 2P only for phase II, as seen in the X-ray data.

Conclusions

The Raman data depict phase transitions in 2P−C_{60} in several ways:

The abrupt H_g modes scattering intensity modifications at ~147 K seem to result from the influence of the triclinic → monoclinic phase transformation on C_{60} electronic transitions, which changes the C_{60} site symmetry. Moreover, the absence of any photodimerization in phases II and III at any laser irradiation duration indicates that the relative orientation of adjacent C_{60} molecules is totally unfavorable to the formation of a chemical bond between them, as in the low-temperature phase of pristine C_{60} where double bonds of one molecule face the center of a hexagon or pentagon of the nearest neighbors. On the contrary, above the monoclinic → monoclinic transition (~212 K) the C_{60} molecules are almost free to rotate in such a way as to have a nonzero probability for adjacent cages to have one of their C=C bonds facing each other; thus, with a power of ~150 W/cm^2, C_{60} dimers are photoinduced for $T > 212$ K.

The main 2P modes are visible in NIR-excited FT-Raman spectra. At least three of them show modifications at the temperatures of the phase transitions. The appearance of the additional ~3055 cm^{-1} mode in the C−H stretching band (3040−3080 cm^{-1}) agrees with the X-ray scattering observation that the 2P molecule passes from an almost planar configuration in phase I ($T > 212$ K) to a configuration in phase II (147−212 K) where the centrosymmetry is lost as a result of the large twisting of the 2P molecule ($\tau \sim 23°$) before returning to a less twisted geometry for $T < 147$ K (phase III).

Acknowledgment. We are happy to acknowledge helpful discussions with R. Moret, P. Launois, and M. Krause. The European Union is acknowledged for financial support through the "*FULPROP*" Training & Mobility Research network (T.M.R.) n. ERBFMRX-CT97-0155 as well as the CNR-PF MSTA II-FREMO project.

References and Notes

(1) Gunnarsson, O. *Rev. Mod. Phys.* **1997**, *69*, 575.
(2) Lynden-Bell, R. M.; Michel, K. H. *Rev. Mod. Phys.* **1994**, *66*, 721.
(3) Tou, H.; Maniwa, Y.; Iwasa, Y.; Shimoda, H.; Mitani, T. *Phys. Rev. B* **2000**, *62*, R775.
(4) Shimoda, H.; Iwasa, Y.; Miyamoto, Y.; Maniwa, Y.; Mitani, T. *Phys. Rev. B* **1996**, *54*, R15653.
(5) Capone, M.; Fabrizio, M.; Castellani, C.; Tosatti, E. *Science* **2002**, *296*, 2364.
(6) Pénicaud, A. *Fullerene Sci. Technol.* **1998**, *6*, 731.
(7) Dresselhaus, M. S.; Dresselhaus, G.; Eklund, P. C. *Science of Fullerenes and Carbon Nanotubes*; Academic Press: New York, 1996.
(8) Pénicaud, A.; Carreon, O. Y.; Perrier, A.; Watkin, D. J.; Coulon, C. *J. Mater. Chem.* **2002**, *12*, 913.
(9) Sun, D.; Reed, C. A. *Chem. Commun.* **2000**, *23*, 2391.
(10) Marucci, A.; Launois, P.; Moret, R.; Pénicaud, A. *Eur. Phys. J. B* **2002**, *26*, 29.
(11) Marucci, A.; Launois, P.; Moret, R.; Palles, D.; Ruani, G.; Pénicaud, A. Proceedings of the XV International Winterschool on Electronic Properties of Novel Materials **2001**, *591*, 153.
(12) Meletov, K. P.; Liarokapis, E.; Arvanitidis, J.; Papagelis, K.; Palles, D.; Kourouklis, G. A.; Ves, S. *Chem. Phys. Lett.* **1998**, *290*, 125.
(13) Yu, R. C.; Tea, N.; Salomon, M. B.; Lorents, D.; Malhotra, R. *Phys. Rev. Lett.* **1992**, *2050*, 219.
(14) Denisov, V. N.; Lipin, A. S.; Mavrin, B. N.; Zakhidov, A. A.; Ruani, G.; Zamboni, R.; Taliani, C. *Synth. Met.* **1994**, *64*, 341.
(15) Hadjiev, V. G.; Rafailov, P. M.; Jantoljak, H.; Thomsen, C.; Kelly, M. K. *Phys. Rev. B* **1997**, *56*.
(16) Rafailov, P. M.; Hadjiev, V. G.; Thomsen, C.; Kamarás, K.; Pekker, S. *Chem. Phys. Lett.* **2000**, *326*, 58.
(17) Zhou, P.; Rao, A. M.; Wang, K. A.; Robertson, J. D.; Eloi, C.; Meier, M. S.; Ren, S. L.; Bi, X. X.; Eklund, P. C.; Dresselhaus, M. S. *Appl. Phys. Lett.* **1992**, *60*, 2871.
(18) Eklund, P. C.; Rao, A. M.; Zhou, P.; Wang, Y.; Holden, J. M. *Thin Solid Films* **1995**, *257*, 185.
(19) Senyavin, V. M.; Davydov, V. A.; Kashevarova, L. S.; Rakhmanina, A. V.; Agafonov, V.; Allouchi, H.; Ceolin, R.; Sagon, G.; Szwarc, H. *Chem. Phys. Lett.* **1999**, *313*, 421.
(20) Puschnig, P.; Ambrosch-Draxl, C.; Heimel, G.; Zojer, E.; Resel, R.; Leising, G.; Kriechbaum, M.; Graupner, W. *Synth. Met.* **2001**, *116*, 327.
(21) Guha, S.; Graupner, W.; Resel, R.; Chandrasekhar, M.; Chandrasekhar, H. R.; Glaser, R.; Leising, G. *Phys. Rev. Lett.* **1999**, *82*, 3625.
(22) Rumi, M.; Zerbi, G. *Chem. Phys.* **1999**, *242*, 123.
(23) Heimel, G.; Puschnig, P.; Cai, Q.; Martin, C.; Zojer, E.; Graupner, W.; Chandrasekhar, M.; Chandrasekhar, H. R.; Ambrosch-Draxl, C.; Leising, G. *Synth. Met.* **2001**, *116*, 163.

(24) Heimel, G.; Cai, Q.; Martin, C.; Puschnig, P.; Guha, S.; Graupner, W.; Ambrosch-Draxl, C.; Chandrasekhar, M.; Leising, G. *Synth. Met.* **2001**, *119*, 371.
(25) Zerbi, G.; Sandroni, S. *Spectrochim. Acta* **1968**, *24A*, 483.
(26) Rafailov, P. M.; Hadjiev, V. G.; Goni, A. R.; Thomsen, C. *Phys. Rev. B* **1999**, *60*, 13351.
(27) Zhou, P.; Dong, Z. H.; Rao, A. M.; Eklund, P. C. *Chem. Phys. Lett.* **1993**, *211*, 337.
(28) Jishi, R. A.; Dresselhaus, M. S.; Dresselhaus, G.; Wang, K. A.; Zhou, P.; Rao, A. M.; Eklund, P. C. *Chem. Phys. Lett.* **1993**, *206*, 187.
(29) Zhu, Q.; Zhou, O.; Coustel, N.; Vaughan, G. B. M.; McCaukey, J. P.; Romanow, W. J.; Fischer, J. E.; Smith, A. B. *Science* **1991**, *254*, 545.
(30) Stephens, P. W.; Mihaly, L.; Wiley: J. B.; Huang, S. M.; Kaner, R. B.; Diederich, F.; Whetten, R. L.; Holczer, K. *Phys. Rev. B* **1992**, *45*, 543.
(31) Zhou, O.; Fischer, J. E.; Coustel, N.; Zhu, Q.; McGhie, A. R.; Romanow, W. J.; McCaukey, J. P.; Smith, A. B.; Cox, D. E. *Nature* **1991**, *351*, 462.
(32) von Laue, L.; Ermark, F.; Gölzhäuser, A.; Haeberlen, U.; Häcker, U. *J. Phys.: Condens. Matter* **1996**, *8*, 3977.